International Journal of Modern Physics E
Vol. 25, No. 9 (2016) 1650067 (15 pages)

DOI: 10.1142/S0218301316500671

World Scientific
www.worldscientific.com

# SO(4) group structure for a motivated QCD Hamiltonian: Analytic and Tamm–Dancoff solutions

Tochtli Yepez-Martinez* and Osvaldo Civitarese†

*Departamento de Fisica, Universidad Nacional La Plata,*
*C.C.67 (1900), La Plata, Argentina*
**yepez@fisica.unlp.edu.ar*
†*osvaldo.civitarese@fisica.unlp.edu.ar*

Peter O. Hess

*Instituto de Ciencias Nucleares,*
*Universidad Nacional Autónoma de México,*
*Ciudad Universitaria, Circuito Exterior S/N,*
*A.P. 70-543, 04510 México, DF México*
*hess@nucleares.unam.mx*

Received 1 July 2016
Accepted 1 August 2016
Published 31 August 2016

Starting from the QCD Hamiltonian written in the canonical Coulomb gauge formalism, we developed a mapping onto an SO(4) representation which is suitable for the description of the QCD spectra at low energies. The mapping does not break the flavor symmetry and it preserves the singlet-colorless structure of the states. We present and discuss the structure of integer and half-integer-spin states with masses below 2 GeV. Finally, we extend the formalism in order to include particle–hole-like correlations in building excitations.

*Keywords*: Symmetries; effective Hamiltonian; many body.

PACS Number(s): 12.38.−t, 12.40.Yx, 21.60.Fw, 12.90.+f

## 1. Introduction

One of the main goals in hadronic physics is to construct effective, low-energy approximations to QCD by finding methods to treat its nonperturbative domain. Lattice QCD (LQCD) calculations,[1–8] performed over the past three decades have shown significant advances in nonperturbative aspects of the fundamental theory of strong interactions, e.g., an amazing agreement with experimental energies reported for the lightest meson and baryon states as well as some heavier states. Until now, LQCD is the only formalism that can handle QCD from first principles

†Corresponding author.

but it is numerically quite involved. On the other hand, progress in other theoretical approaches to low energy QCD has not been as impressive and they have not extracted substantial information from LQCD in order to construct a simple (minimal) solvable Hamiltonian. Fixing-gauge approaches, like treatments in the canonical Coulomb gauge, offer a connection between QCD and the more traditional nonrelativistic many-body problems in nuclear physics.[9–12] Over the years, a number of nonrelativistic or semi-relativistic models describing quarks in hadronic bound states have been proposed. However, the full effect of quark–anti-quark pairs has never been considered because such effects lead to a many-body problem that can only be treated in some approximation. In hadronic models,[13–15] such approximations are typically driven by phenomenological considerations rather than by QCD based features. Within these phenomenological models a number of experimental masses have been considered and reproduced by introducing a large number of parameters. Nevertheless, these kind of models are of interest to illuminate any possible connection between phenomenological models and QCD.

In Refs. 16–18, schematic models for the low-energy quark dynamics were developed with the purpose to capture selective features of the theory within a finite Fock space. The implementation of a contact interaction as a two-body interaction led to the SU(3)-Casimir structure,[19] as well as analytic solutions. Recently, in Ref. 20, a confining interaction corresponding to a more rigorous relation to QCD was investigated, establishing a general picture of the relevant two-body interactions to be analyzed by many-body techniques (e.g., Tamm–Dancoff (TD) and random phase approximations). The later requires to extend the Fock space in order to guarantee convergence of the eigenvalues, making the analysis purely numerical and moving away from a pursued minimal model.

In this paper, we explore a simple effective quark Hamiltonian guided by QCD and examine various classes of solutions that may represent hadronic states. The study is performed in the context of a group structure, the SO(4) group, the generators of which exhibit a strong correspondence with the elements appearing in the QCD Hamiltonian. We then proceed to show that a convenient parametrization of the SO(4) Casimir-forms fits reasonably the low-energy spectrum of QCD, both for mesons and baryons, and write an effective Hamiltonian which encompasses the symmetries of the SO(4) group. Because of the highly nonperturbative structure of QCD, it is rather obvious that we do not pretend to replace the complete QCD Hamiltonian by the effective one based on the SO(4), but we demonstrate that it indeed contains some of the relevant degrees of freedom of QCD at low-energy. Since the many-body aspects of QCD have been explored previously,[10,17,18,20] we also use the TD method,[21] to perform a diagonalization in a basis of pairs and compare our results with experimental data. The paper is organized as follows: The structure of the QCD Hamiltonian is presented in Sec. 2, the mapping onto an SO(4)-representation is discussed in Sec. 3, and the resulting Hamiltonian is shown in Sec. 4. The TD analysis and the discussion of the results are shown in Sec. 5. Finally, our conclusions are presented in Sec. 6.

## 2. The Canonical Representation of the QCD Hamiltonian

The fundamental non-abelian theory of strong interactions, QCD, has been widely studied in its canonical Coulomb gauge representation, Eq. (1).[9,10,17] It was shown in Ref. 10 that two of the main features of QCD, e.g., confinement and the constituent particles (quarks and gluons) can be treated simultaneously in that framework. However, the study of dynamical quarks and gluons and their interactions in the low-energy regime is highly nontrivial, and the use of an effective Hamiltonian, if it becomes available, may help to understand the nonperturbative domain of the theory. The QCD Hamiltonian, in the canonical Coulomb gauge representation, is written

$$H^{\rm QCD} = \int \left\{ \frac{1}{2}[\mathcal{J}^{-1}\Pi_i^{{\rm tr}\,a}\mathcal{J}\Pi_i^{{\rm tr}\,a} + \mathbf{B}_i^a\mathbf{B}_i^a] + \psi^\dagger{}_{cf}(-i\alpha\cdot\nabla + \beta m)\psi_{cf} - g\psi^\dagger{}_{cf}\alpha\cdot\mathbf{A}^a T^a_{cc'}\psi_{c'f} \right\} d\mathbf{r} + \frac{1}{2}g^2\int \mathcal{J}^{-1}\rho^a(\mathbf{r})\left\langle a,\mathbf{r}\left|\frac{1}{\nabla\cdot\mathbf{D}}(-\nabla^2)\frac{1}{\nabla\cdot\mathbf{D}}\right|a'\mathbf{r}'\right\rangle \mathcal{J}\rho^{a'}(\mathbf{r}')d\mathbf{r}d\mathbf{r}'. \quad (1)$$

The transverse chromo-electromagnetic fields in QCD Coulomb gauge are indicated by $\Pi$ and $\mathbf{B}$, while $\psi$ represents the quark fields. The last two terms in Eq. (1) are the quark–gluon interaction ($g$-term) and the quark and anti-quark color charge-densities interaction ($g^2$-term), respectively. The latter is a gauge dependent interaction, coming from the inverse of the Faddeev–Popov term $(\nabla\cdot\mathbf{D})^{-1}$ and its determinant $\mathcal{J} = \det(\nabla\cdot\mathbf{D})$.[9] In the low-energy regime of QCD, light quarks and their interactions play the most important role, and the effects of dynamical gluons may be absorbed in the interaction $V(R) = -\frac{a}{R} + bR$, which is obtained from a self-consistent treatment of the gauge-dependent interaction between color charge densities, as it was shown in Ref. 10. Therefore, one can write, for the effective QCD Hamiltonian, the expression

$$H_{\rm eff}^{\rm QCD} = \int \{\psi^\dagger(\mathbf{r})(-i\alpha\cdot\nabla + \beta m)\psi(\mathbf{r})\}d\mathbf{r} + \frac{1}{2}\int \rho_a(\mathbf{r})V(|\mathbf{r}-\mathbf{r}'|)\rho^a(\mathbf{r}')d\mathbf{r}d\mathbf{r}', \quad (2)$$

where $\rho^a(\mathbf{r}) = \rho_q^a(\mathbf{r}) + \rho_{\bar{q}}^a(\mathbf{r}) = \psi^\dagger(\mathbf{r})T^a\psi(\mathbf{r})$ and $\psi^\dagger(\mathbf{r}) = (\psi_1^\dagger(\mathbf{r},\sigma,c,f),\psi_2^\dagger(\mathbf{r},\sigma,c,f))$, with $\sigma, c, f$ indicating the spin, color and flavor intrinsic degrees of freedom. In order to calculate the spectrum of low-energy mesons, lattice QCD[7,8] and many-body techniques have been applied, mostly numerically, to reproduce certain characteristics of the spectrum. Practically all those approaches fail in reproducing the pion mass. Some of the standard bosonization-methods, like the TD and random phase approximations, have shown to be useful[22] to elucidate the role of the pion as a Goldstone-like state of the theory. Although the many-body methods are much less involved, than lattice calculations, their implementation requires some minimal information i.e., quarks masses, couplings and interactions, about the fundamental degrees of freedom and about the symmetries exhibited by them.

## 3. Mapping to a Simple Model

As mentioned in the previous section, the motivation of this work comes from the side of the effective QCD Hamiltonian, Eq. (2), and the nonperturbative predictive power of many-body methods for the low-energy regime of QCD. The quantized structure of the effective Hamiltonian (2) has been discussed in Ref. 20 and it is given by

$$
\begin{aligned}
H_{\text{eff}}^{\text{QCD}} = & \sum_{\Gamma_1\mu_1} \varepsilon_{\Gamma_1}(b^\dagger_{\Gamma_1\mu_1} b_{\Gamma_1\mu_1} - d_{\Gamma_1\mu_1} d^\dagger_{\Gamma_1\mu_1}) \\
& + \sum_{\Gamma} \sum_{\Gamma_i} \{V_1(\Gamma_i)[([b^\dagger_{\Gamma_1} \otimes b_{\Gamma_2}]^\Gamma - [d_{\Gamma_1} \otimes d^\dagger_{\Gamma_2}]^\Gamma) \otimes ([b^\dagger_{\Gamma_3} \otimes b_{\Gamma_4}]^\Gamma \\
& - [d_{\Gamma_3} \otimes d^\dagger_{\Gamma_4}]^\Gamma)]^{\hat{0}}_{\hat{0}} + V_2(\Gamma_i)[([b^\dagger_{\Gamma_1} \otimes b_{\Gamma_2}]^\Gamma - [d_{\Gamma_1} \otimes d^\dagger_{\Gamma_2}]^\Gamma) \otimes ([b^\dagger_{\Gamma_3} \otimes d^\dagger_{\Gamma_4}]^\Gamma \\
& + [d_{\Gamma_3} \otimes b_{\Gamma_4}]^\Gamma)]^{\hat{0}}_{\hat{0}} + V_3(\Gamma_i)[([b^\dagger_{\Gamma_1} \otimes d^\dagger_{\Gamma_2}]^\Gamma + [d_{\Gamma_1} \otimes b_{\Gamma_2}]^\Gamma) \otimes ([b^\dagger_{\Gamma_3} \otimes b_{\Gamma_4}]^\Gamma \\
& - [d_{\Gamma_3} \otimes d^\dagger_{\Gamma_4}]^\Gamma)]^{\hat{0}}_{\hat{0}} + V_4(\Gamma_i)[([b^\dagger_{\Gamma_1} \otimes d^\dagger_{\Gamma_2}]^\Gamma + [d_{\Gamma_1} \otimes b_{\Gamma_2}]^\Gamma) \\
& \otimes ([b^\dagger_{\Gamma_3} \otimes d^\dagger_{\Gamma_4}]^\Gamma + [d_{\Gamma_3} \otimes b_{\Gamma_4}]^\Gamma)]^{\hat{0}}_{\hat{0}}\}, \qquad (3)
\end{aligned}
$$

where the vacuum state is represented by $|\tilde{0}\rangle$ and it is annihilated by the action of quark and anti-quark, $b_\Gamma$ and $d_\Gamma$, operators respectively, i.e., $b_\Gamma|\tilde{0}\rangle = d_\Gamma|\tilde{0}\rangle = 0$. $\Gamma_i$ is a short hand notation for the irreducible representations of spin, color and flavor. The matrix elements $V_i$ have been explicitly shown in Ref. 20, and they consist of a confining interaction resulting from a Coulomb plus linear potential.

In order to assure basis independence of the observables (eigenvalues) from the diagonalization of the Hamiltonian of (3), the number of configurations ($\Gamma_i$) should be large, but a reduction of the Fock space may provide some insights on the spectrum. To achieve this goal, we have constructed all the possible operators that describe particles of spin-$\frac{1}{2}$, for the specific space shown in Fig. 1. The energy degeneracy between the two lower (upper) states could be viewed also as an isospin degeneration, e.g., up, down and strange quarks masses in an SU(3) group. Such

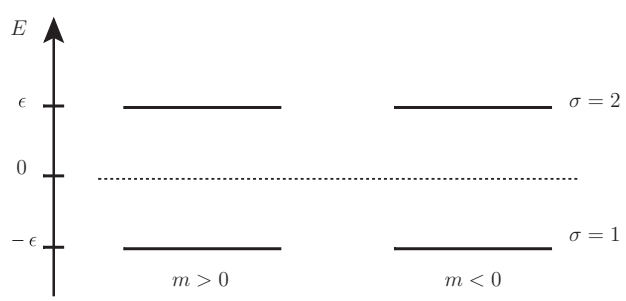


Fig. 1. Model space.

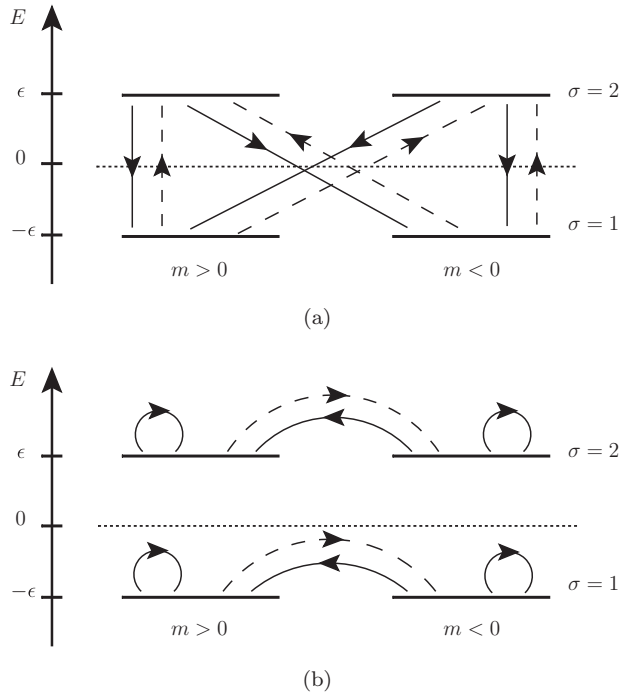


Fig. 2. (a) Rising and lowering of the $\sigma$-value operations. (b) Invariant $\sigma$-value operations.

degeneracy and symmetry can be explicitly broken by introducing another state ($\epsilon_2 > \epsilon > 0$) at higher energy for the strange quark state.

The minimal number of operations in the space of Fig. 1 is 16, and they are shown in Fig. 2, eight of these correspond to rising and lowering the value of $\sigma$, and the other eight leave the value of $\sigma$ invariant. The label $\sigma$ is associated with anti-quark ($\sigma = 1$) and quark ($\sigma = 2$) states. Their color and flavor degrees of freedom are contained in the creation and annihilation operators $C^{\dagger}_{\sigma m}(a, f)$, $C_{\sigma m}(a, f)$, with $a = (G, B, R)$ (color) and $f = (u, d, s)$ (flavor). The minimal model constructed here rely on the fact that physical states are color singlets, and that the states will not be classified by their flavor content (see Sec. 4) since that requires the flavor symmetry being explicitly broken.

All the operations of the subspace are shown in Fig. 2, and they are easily identified within the context of the Hamiltonian of Eq. (3). We order these operations by the action of six operators, which are

$$\begin{aligned} &\hat{A} = \sum_m C^{\dagger}_{2m} C_{1m}, \quad \hat{B} = \sum_m C^{\dagger}_{2m} C_{1-m}, \quad \hat{C} = \hat{A}^{\dagger}, \quad \hat{D} = \hat{B}^{\dagger}, \\ &\hat{E} = \sum_{\sigma,m} \frac{(-1)^{\sigma}}{2} C^{\dagger}_{\sigma m} C_{\sigma m}, \quad \hat{F} = \sum_{\sigma,m} \frac{(-1)^{\sigma}}{2} C^{\dagger}_{\sigma m} C_{\sigma -m}, \end{aligned} \tag{4}$$

Table 1. Commutators of the operators (4).

| Op. | $\hat{A}$ | $\hat{B}$ | $\hat{C}$ | $\hat{D}$ | $\hat{E}$ | $\hat{F}$ |
|---|---|---|---|---|---|---|
| $\hat{A}$ | 0 | 0 | $2\hat{E}$ | $2\hat{F}$ | $-\hat{A}$ | $-\hat{B}$ |
| $\hat{B}$ | 0 | 0 | $2\hat{F}$ | $2\hat{E}$ | $-\hat{B}$ | $-\hat{A}$ |
| $\hat{C}$ | $-2\hat{E}$ | $-2\hat{F}$ | 0 | 0 | $\hat{C}$ | $\hat{D}$ |
| $\hat{D}$ | $-2\hat{F}$ | $-2\hat{E}$ | 0 | 0 | $\hat{D}$ | $\hat{C}$ |
| $\hat{E}$ | $\hat{A}$ | $\hat{B}$ | $-\hat{C}$ | $-\hat{D}$ | 0 | 0 |
| $\hat{F}$ | $\hat{B}$ | $\hat{A}$ | $-\hat{D}$ | $-\hat{C}$ | 0 | 0 |

where we have omitted color and flavor indexes and written $C^{\dagger}_{\sigma m}(a,f) = C^{\dagger}_{\sigma m}$, keeping the magnetic projection $m$. The commutators $[\hat{O}_1, \hat{O}_2]$, for the set of operators (4), are given in Table 1.

The SO(4) group turns out to be the group that satisfies this algebra, as it is explained next.

### 3.1. *Rising and lowering operators of the* SO(4) *group*

The SO(4) group algebra[23] is given by

$$\begin{aligned} [\hat{J}_i, \hat{J}_j] &= i\epsilon_{ijk}\hat{J}_k, \\ [\hat{J}_i, \hat{V}_j] &= i\epsilon_{ijk}\hat{V}_k, \\ [\hat{V}_i, \hat{V}_j] &= i\epsilon_{ijk}\hat{J}_k. \end{aligned} \tag{5}$$

Instead of using the Cartesian components $J_i, V_i$, it is more convenient to use $J_{\pm}, J_0$ and $V_{\pm}, V_0$ defined by

$$\hat{J}_+ = \hat{J}_1 + i\hat{J}_2, \quad \hat{J}_- = \hat{J}_1 - i\hat{J}_2, \quad \hat{J}_0 = \hat{J}_3 \tag{6}$$

and

$$\hat{V}_+ = \hat{V}_1 + i\hat{V}_2, \quad \hat{V}_- = \hat{V}_1 - i\hat{V}_2, \quad \hat{V}_0 = \hat{V}_3, \tag{7}$$

respectively. With the algebra of Eq. (5) and the commutators of Table 1, the operators defined in Eq. (4) are identified to the ones of the SO(4) group (6) and (7) by

$$\begin{aligned} \hat{A} = \hat{J}_+, \quad \hat{C} = \hat{J}_-, \quad \hat{E} = \hat{J}_0, \\ \hat{B} = \hat{V}_+, \quad \hat{D} = \hat{V}_-, \quad \hat{F} = \hat{V}_0. \end{aligned} \tag{8}$$

### 3.2. *Casimir operators of SO*(4)

The SO(4) group has two invariant operators, $\hat{\mathcal{C}}_1$ and $\hat{\mathcal{C}}_2$, which commute with all the generators

$$\begin{aligned} \hat{\mathcal{C}}_1 &= \hat{\mathbf{J}}^2 + \hat{\mathbf{V}}^2 = \hat{J}_+\hat{J}_- + \hat{V}_+\hat{V}_- + \hat{V}_0^2 + \hat{J}_0(\hat{J}_0 - 2), \\ \hat{\mathcal{C}}_2 &= \hat{\mathbf{J}} \cdot \hat{\mathbf{V}} = \frac{1}{2}(\hat{J}_-\hat{V}_+ + \hat{J}_+\hat{V}_-) + \hat{J}_0\hat{V}_0. \end{aligned} \tag{9}$$

Having identified the SO(4) group for the algebra of the operators of Eq. (4), and motivated by the quantized Hamiltonian of QCD, Eq. (3), it seems feasible to grasp some relevant characteristics of QCD within a simple model based on SO(4) group operators.

## 4. SO(4) Hamiltonian

In this section, we introduce the SO(4) Hamiltonian constructed from the generators and Casimir operators introduced in the previous section. Therefore, in analogy to the many-body problem in low energy QCD, described in Sec. 3, the Hamiltonian acting on the space shown in Fig. 1, can be written as

$$\begin{aligned} H &= \sum_m \epsilon(C^\dagger_{2m}C_{2m} - C^\dagger_{1m}C_{1m}) + a_{M(B)}\hat{\mathcal{C}}_1 + b_{M(B)}\hat{\mathcal{C}}_2 \\ &= 2\epsilon\hat{J}_0 + a_{M(B)}\hat{\mathcal{C}}_1 + b_{M(B)}\hat{\mathcal{C}}_2, \end{aligned} \tag{10}$$

where the subscripts $M(B)$ indicate the meson(baryon) couplings, which in general are expected to be different, while $\epsilon$ is expected to be independent of the state, since it corresponds to the single particle term without interactions, i.e., the free Dirac term. It is worth to remember that each particle created and/or annihilated by the operators $C^\dagger_{\sigma m}, C_{\sigma m}$ has nine possibilities associated with the combinations of color and flavor degrees of freedom.

In Ref. 23, the SO(4) group algebra as well as its irreducible representations $(j_0, \eta)$ have been analyzed. Here, we just consider the possible representations $(j_0, \eta)$ that could be involved in the meson and baryon spectrum of Eq. (10) and make a fit to the set of parameters, $a_{M(B)}$ and $b_{M(B)}$, to experimental values. A short review of SO(4) $(j_0, \eta)$-representations is shown in Appendix A.

### 4.1. *Integer spin*: $J = 0, 1$ *states*

The low-energy spectrum of meson ($J = 0, 1$) and baryon ($J = \frac{1}{2}, \frac{3}{2}$) states can be obtained within this model by looking at the excitations of the model and the quantum numbers associated to them. To elucidate the occurrence of pseudo-scalar ($J = 0$) and vector ($J = 1$) states in SO(4), the simplest way to proceed is by direct identification. The allowed irreducible representations (irreps) are shown in Table 2.

Table 2. SO(4) representations associated with the pseudo-scalar and vector states.

| $(J, M_J)$ | $(j_0, \eta)$ | $(j_0, \eta)$ |
|---|---|---|
| (0,0) | (0,1) | (0,2) |
| $(1, M_J)$ | (0,2) | ($\pm$1,2) |

The meson-like eigenvalues of the Hamiltonian of Eq. (10), for the states $|(j_0,\eta);JM_J\rangle$ of Table 2, are described by the following combinations:

$$\begin{aligned}
|(0,1);00\rangle &\to E=0,\\
|(0,2);00\rangle &\to E=3a_M,\\
|(0,2);1M_J\rangle &\to E=2\epsilon M_J+3a_M,\\
|(\pm1,2);1M_J\rangle &\to E=2\epsilon M_J+4a_M-2b_M\\
&\quad =2\epsilon M_J+3a_M+(a_M-2b_M).
\end{aligned} \tag{11}$$

By construction $\epsilon\neq 0$, which is related with the explicit chiral symmetry breaking of the quarks and it plays the role of the free Dirac term. Since we are assuming an exact symmetry for the flavor group, i.e., the SU(3) group, all the masses of the quarks are considered to be equal but small, so that, one can choose an average value for the three lowest quark masses in order to assign a value for $\epsilon$. In fact, here we show that this is the case for the model and it comes out naturally by analyzing the small splitting in the mass of the mesons with $J=0,1$, as well as in the baryon $J=\frac{1}{2},\frac{3}{2}$ sector, see Sec. 4.2. By a simple analysis of the eigenvalues, (11), it seems natural to associate the $(0,1)$ SO(4) representation with the pion state. Since the factor $3a_M$ appears in both the pseudo-scalar and the vector states, it seems also natural to associate the factor $a_M-2b_M$ with a mass-splitting within the $J=1$ vector meson sector.

In the following calculation, we consider the pseudo-scalar and vector mesons with masses about 1 GeV. Obviously the fit will have some discrepancies with experimental masses since we are not considering the flavor symmetry breaking. Nevertheless, as it will be shown below, the meson and baryon predictions of this simple model for energies around the 1 GeV are satisfactory, in spite of the fact of the just mentioned lack of the flavor symmetry breaking.

The simplest relations of the couplings $a_M, b_M$ with the physical states are

$$\begin{aligned}
2\epsilon|M_J| &= \frac{1}{2}(M_\rho+M_\omega)-\frac{1}{3}(M_\eta+M_{\eta'}+M_K)=108.40\,\text{MeV},\\
3a_M &= \frac{1}{5}((M_\rho+M_\omega)+(M_\eta+M_{\eta'}+M_K))=710.96\,\text{MeV},\\
a_M-2b_M &= M_\phi-\frac{1}{3}(M_\rho+M_\omega+M_{K^*})=205.33\,\text{MeV},
\end{aligned} \tag{12}$$

which leads to $\epsilon=54.20\,\text{MeV}$, $a_M=236.98\,\text{MeV}$ and $b_M=15.82\,\text{MeV}$. The pseudo-scalar and vector masses have been taken from Ref. 24. The comparison of the energy eigenvalues of the SO(4) representations with the experimental data is shown in Fig. 3.

From the results displayed in Fig. 3, it is seen that physical states $(J,M_J)$ may be labeled by SO(4) $(j_0,\eta)$-irreps. A closer correspondence with the experimental

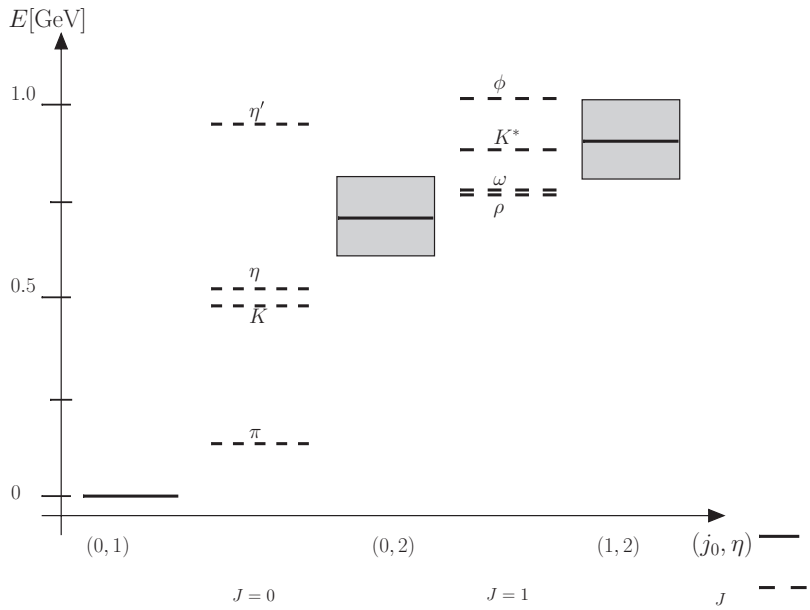


Fig. 3. Comparison of the energy spectrum for the physical pseudo-scalar and vector states (dashed-lines) and the SO(4) representations (solid-lines). The shadowed boxes measure the spreading of the eigenvalues due to the presence of the single-particle term $2\epsilon\hat{J}_0$ in (10).

energies may require additional corrections coming from, e.g., SU(3) flavor symmetry breaking, vacuum-correlations induced by pairs. A few words can be added concerning the effects of color degrees of freedom on the SO(4) eigenvalues. Since physical states contained in such representations must be colorless, and in the absence of gluonic degrees of freedom, only the combinations $G\bar{G}, B\bar{B}, R\bar{R}$ are possible for the meson sector.

### 4.2. *Half-integer spin* $J = \frac{1}{2}, \frac{3}{2}$ *states*

The half-integer states of the low-energy baryon spectrum correspond to spin $J = \frac{1}{2}$ and $\frac{3}{2}$. The SO(4) representations that contain these states are given in Table 3.

Table 3. SO(4) representations associated with the half-integer states $J = \frac{1}{2}, \frac{3}{2}$.

| $(J, M_J)$ | $(j_0, \eta)$ | $(j_0, \eta)$ |
|---|---|---|
| $(\frac{1}{2}, M_J)$ | $(\pm\frac{1}{2}, \frac{3}{2})$ | $(\pm\frac{1}{2}, \frac{5}{2})$ |
| $(\frac{3}{2}, M_J)$ | $(\pm\frac{1}{2}, \frac{5}{2})$ | $(\pm\frac{3}{2}, \frac{5}{2})$ |

The baryon eigenvalues of the Hamiltonian of Eq. (10), for the half-integer states $|(j_0,\eta);JM_J\rangle$ of Table 3, are given by the following linear combinations:

$$\begin{aligned}
&\left|\left(\pm\frac{1}{2},\frac{3}{2}\right);\frac{1}{2}\pm\frac{1}{2}\right\rangle \rightarrow E_1=\pm\epsilon+\epsilon_1,\\
&\left|\left(\pm\frac{1}{2},\frac{5}{2}\right);\frac{1}{2}\pm\frac{1}{2}\right\rangle \rightarrow E_2=E_1+\Delta_1,\\
&\left|\left(\pm\frac{1}{2},\frac{5}{2}\right);\frac{3}{2}M_J\right\rangle \rightarrow E_3=2\epsilon\left(M_J\mp\frac{1}{2}\right)+E_2,\\
&\left|\left(\pm\frac{3}{2},\frac{5}{2}\right);\frac{3}{2}M_J\right\rangle \rightarrow E_4=2\epsilon M_J+5\epsilon_1.
\end{aligned} \tag{13}$$

with

$$\begin{aligned}
\epsilon_1&=\frac{3}{2}\left(a_B-\frac{1}{2}b_B\right),\\
\Delta_1&=4a_B-\frac{1}{2}b_B
\end{aligned} \tag{14}$$

and $E_3-E_2=\pm 2\epsilon$ for $M_J=\pm\frac{3}{2}$ and $E_3-E_2=0$ for $M_J=\pm\frac{1}{2}$. By fitting the observed masses, one can now determine the parameters of the model for each of the states. However, the task is not so simple as it was for the case of mesons, because of the large separation between lowest and highest energy states in the SO(4) irrep. From (13), the ratio $(E_4-2\epsilon M_J)/(E_1\mp\epsilon)$ yields a factor of the order of 5 between the lowest and highest baryon states, regardless of their structure. By looking at the experimental data for $J=\frac{1}{2},\frac{3}{2}$, the ratio is smaller, e.g., $M_\Omega/M_{p,n}\approx 2$.

In view of this discrepancy, it seems natural to fit the lowest SO(4) representation $(\pm\frac{1}{2},\frac{3}{2})$ at the average energy of the proton and neutron masses $E_1\mp\epsilon=\epsilon_1=\frac{1}{2}(M_p+M_n)$ and set the value of $\epsilon$ to fit the difference between the closest masses of the $J=\frac{1}{2}$ and $J=\frac{3}{2}$ irreps, like in the pseudo-scalar mesons case, while for the energy gap $\Delta_1$, the value is set as the difference between the average energies of the $J=\frac{1}{2}$ and $J=\frac{3}{2}$ states.

$$\begin{aligned}
2\epsilon&=\frac{M_{\Sigma^*}+M_\Delta}{2}-\frac{M_{\Lambda^0}+M_\Sigma+M_\Xi}{3}=101.3\,\text{MeV},\\
\Delta_1&=\frac{M_\Omega+M_{\Xi^*}+M_{\Sigma^*}+M_\Delta}{4}-\frac{M_\Xi+M_\Sigma+M_{\Lambda^0}+M_n+M_p}{5}\\
&=354.89\,\text{MeV},
\end{aligned} \tag{15}$$

so that $\epsilon=50.65\,\text{MeV}$, $a_B=-90.32\,\text{MeV}$ and $b_B=-1432.38\,\text{MeV}$.

It is worth to mention that in performing the present calculations, several combinations of masses where used in order to fit the factor $\Delta_1$. The results showed that the energy $E_2$ lies in between the energy scale of the $\Lambda$ and $\Omega$ baryons. In Fig. 4, we show the fit that better reproduces the physical states.

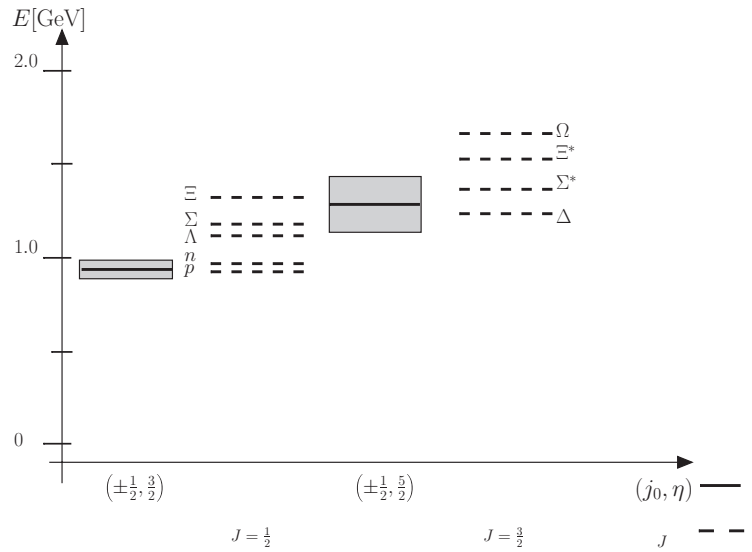


Fig. 4. Energy spectrum for the spin $\frac{1}{2}$ and $\frac{3}{2}$ states belonging to the SO(4) representations.

## 5. Generalization to a More Physical Hamiltonian

By taking the Casimir structure of Eq. (10) as the starting point, we have constructed a more general Hamiltonian for the space of Fig. 1, and calculated its spectrum by applying the TD many-body method to write linear combinations of particle–hole pairs as physical states. This allows us to get some insights on the matrix elements of the effective QCD Hamiltonian (3). In this section, we shall compare the solutions of the TD method with those of the SO(4) Casimir of the previous section.

The Hamiltonian has the structure

$$H = 2\epsilon\hat{J}_0 + \frac{a_1}{2}(\hat{J}_+\hat{J}_- + \hat{V}_+\hat{V}_-) + a_2\hat{V}_0^2 + a_3\hat{J}_0^2 - 2a_4\hat{J}_0 + \frac{a_5}{2}(\hat{J}_+\hat{V}_- + \hat{V}_+\hat{J}_-) + a_6\hat{V}_0\hat{J}_0 - a_7\hat{V}_0, \tag{16}$$

where we have explicitly requested $H^\dagger = H$ just by using $[\hat{J}_-, \hat{V}_+] = -2\hat{V}_0$. Thus, the TD matrix method applied to the Hamiltonian (16) yields

$$A_{ab,a'b'} = \langle\tilde{0}|[\gamma_{a',b'}, [H, \gamma^\dagger_{a,b}]]|\tilde{0}\rangle, \tag{17}$$

with $\gamma^\dagger_{a,b} = C^\dagger_{2m_a}C_{1m_b}$. Therefore, the TD matrix to be diagonalized is defined by

$$A_{a'b',ab} = \Big(2\epsilon - 2a_4 + a_1 + \frac{a_3}{2}\Big)\delta_{m_{a'},m_a}\delta_{m_{b'},m_b} + \Big(\frac{a_2}{4} - \frac{a_6}{2} - a_7\Big)\delta_{m_{a'},m_a}\delta_{m_{b'},-m_b} + \Big(\frac{a_2}{4} + a_5 - a_7\Big)\delta_{m_{a'},-m_a}\delta_{m_{b'},m_b}, \tag{18}$$

as shown in Appendix B. The eigenvalues are given by

$$\begin{aligned} E_1 &= \frac{1}{2}(2a_1 + a_3 - 4a_4 - 2a_5 - a_6 + 4\epsilon), \\ E_2 &= \frac{1}{2}(2a_1 + a_3 - 4a_4 + 2a_5 + a_6 + 4\epsilon), \\ E_3 &= \frac{1}{2}(2a_1 + a_2 + a_3 - 4a_4 + 2a_5 - a_6 - 4a_7 + 4\epsilon), \\ E_4 &= \frac{1}{2}(2a_1 - a_2 + a_3 - 4a_4 - 2a_5 + a_6 + 4a_7 + 4\epsilon). \end{aligned} \tag{19}$$

The correct order of the energies may then be determined by fixing the values of the parameters $\{\epsilon, a_1, a_2, a_3, a_4, a_5, a_6\}$, such that the energies $E_i > 0$ and the gaps between them are constrained to the desired accuracy. In Table 4, we show two sets of parameters which yield very good agreement with the experimental data. In Fig. 5, we show the solutions obtained with the first set of parameters of Table 4 and compare the results with the available data.

Table 4. Parameters and TD energies $E_i$ [MeV].

| Set | $\epsilon$ | $a_1$ | $a_2$ | $a_3$ | $a_4$ | $a_5$ | $a_6$ | $a_7$ | $E_1$ | $E_2$ | $E_3$ | $E_4$ |
|---|---|---|---|---|---|---|---|---|---|---|---|---|
| 1 | 60 | 300 | −100 | 200 | −50 | 200 | −100 | −100 | 470 | 770 | 1020 | 220 |
| 2 | 120 | 200 | 100 | 300 | −50 | 300 | 100 | 100 | 340 | 1040 | 790 | 590 |

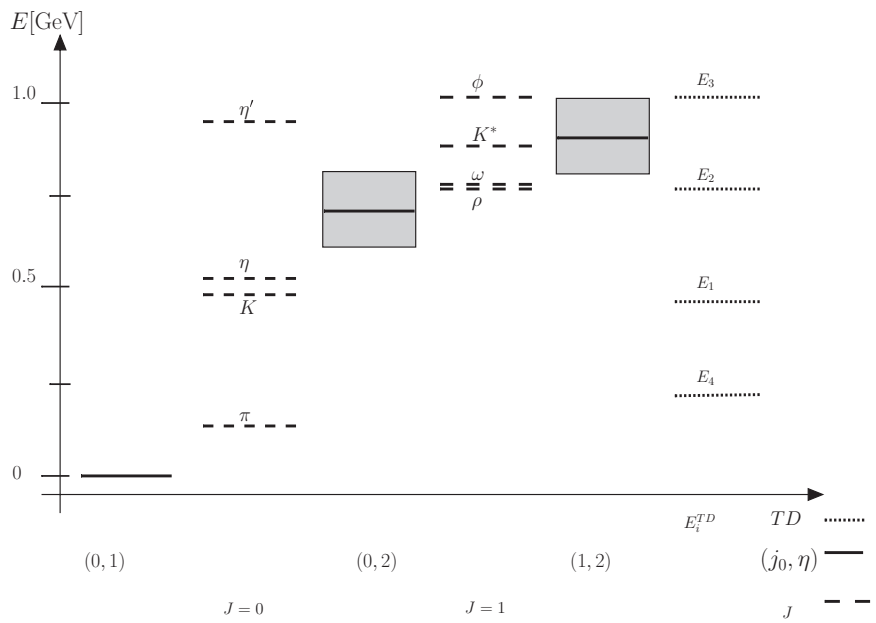


Fig. 5. Comparison of the SO(4) (solid-line), TD (dotted-line) and experimental (dashed-line) energies.

## 6. Summary

In this work, we have explored some of the symmetries exhibited by the QCD Hamiltonian, written in the canonical Coulomb gauge representation. We found that the SO(4) group structure seems to host a significant number of features associated to the lowest QCD energy meson and baryon states. The generators of the SO(4) group, and the associate Casimir operators, seems to represent rather satisfactorily the structure of $J = \frac{1}{2}, \frac{3}{2}, 1, 2$ states as well as the pion state. The analysis based on the SO(4) group structure was extended to include particle–hole-like correlations, by means of the TD approach. The inclusion of these correlations improves significantly the agreement with data. We may then conclude our analysis by stressing the value of the use of standard many-body techniques to explore the extremely rich, and complicated, structure of QCD in the nonperturbative regime. As shown here, we have started from a rigorously-formulated QCD Hamiltonian, mapped it onto a group representation and found that, under the assumption of flavor conservation, the masses of physical colorless states below 2 GeV are in correspondence with the eigenvalues predicted by the SO(4) group. Then, we have shown that the results are improved by adding correlations. The use of these concepts may allow us to better understand, gradually, the structure of physical states belonging to the QCD scheme. Work is in progress concerning the use of other bosonization methods.[25]

## Acknowledgments

One of the authors (T.Y-M) thanks the National Research Council of Argentina (CONICET) for a post-doctoral scholarship. O.C. is a member of the scientific career of the CONICET. P.O.H acknowledges financial help from DGAPA-PAPIIT (IN100315) and from CONACYT (Mexico, Grant 251817). This work has been supported financially by the CONICET (PIP-282) and by the ANPCYT.

## Appendix A. A Review of the SO(4) Group (Ref. 23)

The eigenvalues of the SO(4) Casimir operators are given by

$$\begin{aligned} \hat{\mathcal{C}}_1|(j_0,\eta);jm\rangle &= (j_0^2+\eta^2-1)|(j_0,\eta);jm\rangle, \\ \hat{\mathcal{C}}_2|(j_0,\eta);jm\rangle &= -j_0\eta|(j_0,\eta);jm\rangle, \end{aligned} \tag{A.1}$$

where

$$2j_0 \in \mathbb{Z}, \quad \eta = |j_0|+1, |j_0|+2, \ldots \tag{A.2}$$

and the space that contain all the allowed values of $j$ is

$$\begin{aligned} R(j_o,\eta) = \{&|(j_0,\eta);jm\rangle;\ j = |j_0|, |j_0|+1, \ldots, \eta-1; \\ &m = -j, -j+1, \ldots, j-1, j\}. \end{aligned} \tag{A.3}$$

The dimension of the $(j_0,\eta)$ representations is

$$\dim(R(j_o,\eta)) = \eta^2 - |j_0|^2. \tag{A.4}$$

## Appendix B. The TD Approximation

The TD method defines collective pairs $\Gamma_n^\dagger$ as a linear combination of the elementary pairs. In this model, an elementary pair is constructed by $C_{2m}^\dagger C_{1m'}$ acting on the vacuum $|\tilde{0}\rangle$. The collective pair is given by

$$\Gamma_n^\dagger = \sum_{m_a m_b} X^n_{m_a,m_b} C^\dagger_{2m_a} C_{1m_b}. \tag{B.1}$$

The index $n$ labels the collective state, it runs from one to the number of elementary pairs. The diagonalization in the basis of pairs of the matrix equation

$$\sum_{m_a,m_b} M_{m_{a'}m_{b'},m_a,m_b} X^n_{m_a m_b} = E_n^{TD} X^n_{m_{a'}m_{b'}}, \tag{B.2}$$

with

$$M_{m_{a'}m_{b'},m_a m_b} = \langle\tilde{0}|[C^\dagger_{1m_{b'}} C_{2m_{a'}}, [H, C^\dagger_{2m_a} C_{1m_b}]]|\tilde{0}\rangle, \tag{B.3}$$

is equivalent to the equation of motion

$$\langle\tilde{0}|[\hat{\Gamma}_{n'}, [H, \hat{\Gamma}_n^\dagger]]|\tilde{0}\rangle = E_n^{TD}\delta_{nn'}, \tag{B.4}$$

which yields a linear expression for the Hamiltonian in the basis of correlated pairs.

### B.1. *Relevant commutators*

So that, first we calculate the commutator $[H, \Gamma_n^\dagger]$ using the results

$$\begin{aligned}
&[\hat{J}_0, \Gamma_n^\dagger] = \Gamma_n^\dagger,\\
&[\hat{J}_+, \Gamma_n^\dagger] = 0,\\
&[\hat{J}_-, \Gamma_n^\dagger] = \sum_{m_a m_b} X^n_{m_a m_b}(C^\dagger_{1m_a} C_{1m_b} - C^\dagger_{2m_a} C_{2m_b}),\\
&[\hat{V}_0, \Gamma_n^\dagger] = \sum_{mm'} X^n_{m_a m_b} \frac{1}{2}(C^\dagger_{2-m_a} C_{1m_b} + C^\dagger_{2m_a} C_{1-m_b}),\\
&[\hat{V}_+, \Gamma_n^\dagger] = 0\\
&[\hat{V}_-, \Gamma_n^\dagger] = \sum_{m_a m_b} X^n_{m_a m_b}(C^\dagger_{1-m_a} C_{1m_b} - C^\dagger_{2m_a} C_{2-m_b}).
\end{aligned} \tag{B.5}$$

Then for the Hamiltonian of Eq. (16), we have

$$\begin{aligned}
[H, \Gamma_n^\dagger] = 2(\epsilon - a_4)[\hat{J}_0, \hat{\Gamma}_n^\dagger] + \frac{a_1}{2}[\hat{J}_+\hat{J}_- + \hat{V}_+\hat{V}_-, \hat{\Gamma}_n^\dagger] + a_2[\hat{V}_0^2, \hat{\Gamma}_n^\dagger] + a_3[\hat{J}_0^2, \hat{\Gamma}_n^\dagger]\\
+ \frac{a_5}{2}[\hat{J}_+\hat{V}_- + \hat{J}_-\hat{V}_+, \hat{\Gamma}_n^\dagger] + a_6[\hat{V}_0\hat{J}_0, \hat{\Gamma}_n^\dagger] - a_7[\hat{V}_0, \hat{\Gamma}_n^\dagger],
\end{aligned} \tag{B.6}$$

leading to

$$\langle\tilde{0}|[\hat{\Gamma}_{n'}, [H, \Gamma_n^\dagger]]|\tilde{0}\rangle = \sum_{\{m's\}} (X^{n'}_{m_{a'},m_{b'}})^\dagger\{\cdots\}X^n_{m_a,m_b}, \tag{B.7}$$

with

$$\begin{aligned}\{\cdots\} = &\Big(2\epsilon - 2a_4 + a_1 + \frac{a_3}{2}\Big)\delta_{m_{a'},m_a}\delta_{m_{b'},m_b} \\ &+ \Big(\frac{a_2}{4} - \frac{a_6}{2} - a_7\Big)\delta_{m_{a'},m_a}\delta_{m_{b'},-m_b} \\ &+ \Big(\frac{a_2}{4} + a_5 - a_7\Big)\delta_{m_{a'},-m_a}\delta_{m_{b'},m_b}. \end{aligned} \tag{B.8}$$

## References


1. J. Engels, F. Karsch, H. Satz and I. Montvay, *Nucl. Phys. B* **205** (1982) 545.
2. G. Boyd *et al.*, *Nucl. Phys. B* **469** (1996) 419.
3. K. J. Juge, J. Kuti and C. J. Morningstar, *Nucl. Phys. B, Proc. Suppl.* **63** (1998) 326.
4. P. de Forcrand and M. D'Elia, *Phys. Rev. Lett.* **82** (1999) 4582.
5. J. J. Dudek, R. G. Edwards and D. G. Richards, *Phys. Rev. D* **73** (2006) 074507.
6. G. Burgio, M. Quandt and H. Reinhardt, *Phys. Rev. Lett.* **102** (2009) 032002.
7. QCDSF-UKQCD Collab. (W. Bietenholz *et al.*), *Phys. Rev. D* **84** (2011) 054509.
8. J. Dudek, *Phys. Rev. D* **84** (2011) 074023.
9. T. D. Lee, *Particle Physics and Introduction to Field Theory* (Harwood, Academic New York, 1981).
10. A. P. Szczepaniak and E. S. Swanson, *Phys. Rev. D* **65** (2001) 025012.
11. C. Feuchter and H. Reinhardt, *Phys. Rev. D* **70** (2004) 105021.
12. D. Epple, H. Reinhardt and W. Schleifenbaum *Phys. Rev. D* **75** (2007) 045011.
13. T. DeGrand, R. L. Jaffe, K. Johnson and J. Kiskis, *Phys. Rev. D* **12** (1975) 2060.
14. W. Greiner, S. Schramm and E. Stein, *Quantum Chromodynamcis* (Spiriner, Heidelberg, 2002).
15. N. Isgur and G. Karl, *Phys. Rev. D* **18** (1978) 4187.
16. P. O. Hess and A. P. Szczepaniak, *Phys. Rev. C* **73** (2006) 025201.
17. T. Yepez-Martinez, P. O. Hess, A. P. Szczepaniak and O. Civitarese, *Phys. Rev. C* **81** (2010) 045204.
18. T. Yepez-Martinez, A. Amor, P. O. Hess, A. P. Szczepaniak and O. Civitarese, *Int. J. Mod. Phys. E* **20** (2011) 192–199.
19. J. Escher and J. P. Draayer, *J. Math. Phys.* **39** (1998) 5123.
20. D. A. Amor Quiroz, P. O. Hess, O. Civitarese and T. Yepez-Martinez, *J. Phys. Conf. Ser.* **639** (2015) 012014.
21. P. Ring and P. Schuck, *The Nuclear Many Body Problem* (Springer, Heidelberg, 1980).
22. F. J. Llanes-Estrada and S. R. Cotanch, *Phys. Rev. Lett.* **84** (2000) 1102.
23. A. Bohm, *Quantum Mechanics*: *Foundations and Applications* (Springer, Berlin and New York, 1993).
24. Particle Data Group (J. Beringer *et al.*), *Phys. Rev. D* **86** (2012) 010001.
25. T. Yepez-Martinez, A. Amor-Quiroz, P. O. Hess and O. Civitarese, to be published.